GRANULAR MODELING AND SIMULATION FOR POWDER COMPACTION AND FLOWABILITY EVALUATION

TATSUHIKO AIZAWA, S. TAMURA AND J. KIHARA
Department of Metallurgy, University of Tokyo
7-3-1 Hongo, Bunkyo-ku, Tokyo 113, JAPAN

ABSTRACT

New granular modeling has been proposed and developed to make simulation of powder compaction for flowability evaluation. To realize the computer aided design for powder forming, a granular simulation system has been created: Preprocessor to provide adequate granular model alignment, Numerical solver to trace time histories of element configuration and stress transfer, and Postprocessor to evaluate thus calculated results. For numerical examples have been taken several densification and compaction problems to demonstrate the validity and effectiveness of our developing approach.

INTRODUCTION

In the recent fabrication of advanced materials and mechanical members and parts, the powder forming together with the powder metallurgy becomes an essential methodology of processing both for metallic and ceramic materials: 1) Such complex shaped steel parts as gears are produced by sizing and resizing press, 2) Use of CIP, Hot-press and HIP becomes a conventional procedure to make near-net shaping of ceramics [1]. To improve the accuracy of geometric configuration and to make good quality assurance, we need precise description of mechanical behaviors of powders or granules and require for reliable prediction of mechanical properties and their changes in powder forming. The first approach of mechanical modeling for powders was based on the continuum mechanics; several constitutive equations have been proposed to take into account the effect of porosity structure to powder mechanical response [2,3,4,5]. In Reference 5] was discussed the effect of static pressure to the yield criterion: the yielding function Y is dependent both on the stress deviator S_{ij} and the pressure p in the following functional form.

$$Y = (1/2)S_{ij}S_{ij} + (1/3F^2)p^2 - (1/3)(1-f)^n \sigma_y^2 \quad , \tag{1}$$

and

$$F = (1/a)\, f^b \quad , \tag{2}$$

where f is the porosity fraction to be determined in evolution, σ_y the yield stress of matrix materials and a, b and n are materials constants to be obtained by experiments. Although the partial influence of porosity and powder particle structures on the mechanical behaviors of powders is implicitly considered in the above approach, distinct relation between configuration change of powder particles and flowability in powder forming can be never recognized in the frame of continuum mechanics. Furthermore, the materials constants appearing in the constitutive equations must be determined by multi-axial compression testings, which are often

costly and difficult to obtain objective or indifferent materials relations to such local powder compaction behaviors as observed in the branching or arching phenomena. In other words, since mechanical behaviors observed in those testings are strongly dependent on the powder behaviors intrinsic to each testing condition, little or no constitutive relations can be obtained to describe neutrally the mechanical behaviors of the current powder materials.

Various alternative approaches have been in research on the basis of the discrete modeling [6,7,8,9]: typical distinct element modeling was first developed by Cundall [6] to deal with sand or rock behaviors in civil engineering. Although those related works could be theoretically cited in construction of powder particle models, new modeling is indispensable to describe the fundamental behaviors of powder. Authors [10,11,12,13,14,15] have been concerned with the granular modeling to represent powder and powder-like particles or granules and the reconstruction of equivalent continuum modeling to current powder mechanics. Through those studies have been found that the continuum mechanics model can be applicable when the density of powders becomes sufficiently high in HIP processing and that our developing approach should be useful in dealing with evaluation of powder particle flow and compaction in mechanical pressing or CIP processing.

In the present paper, our developing system of powder forming simulation will be discussed with some comments on the promising functions of processors, mechanical items of powder mechanics and powder characterization. Two mechanical problems will be taken for numerical examples: static compression in quasi-isotropic and uniaxial cases and vibration compaction. In the former, powder particle rearrangement will be discussed with porosity structure and flowability: regular element alignment with statistically distributed grain size can be considered in the initial element generation. In the latter, the effect of powder structure on the flowability will be considered for the applied vibrational force: direct observation of the change of particle configuration helps us to understand the flowability. Through these numerical simulations will be investigated the actual granular modeling.

GRANULAR MODELING

In the granular modeling, the powder particles or granules are represented by an assembly of the rigid circular or spherical elements as illustrated in Fig. 1. Both the grain size distribution and the compaction procedure are explicitly taken into account in the initial element alignments. Fig. 2 lists various element alignments: a) Regular distribution, b) Normal distribution, c) Logarithmic normal distribution, and d) Natural distribution due to gravity compaction. Direct consideration of such applied external forces as gravity or vibration loading leads to actual evaluation of powder structures in forming.

In the present granular modeling, each powder particle is represented by a rigid disc or sphere for two or three dimensional situations, respectively. Two dimensional element has three degrees of freedom: two in the parallel movement along x and y axes and one in the rotation, as shown in Fig. 3(a). These elements can be directly combined with each other to represent various granular elements with larger size and heterogeneous geometry or complex surface geometry, as shown in Fig. 3(b). This allows us to consider the effect of surface geometric structure on the mechanical behaviors.

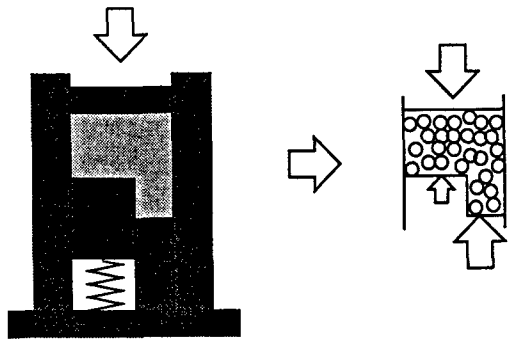

Fig. 1 Representation of powder forming by granular modeling.

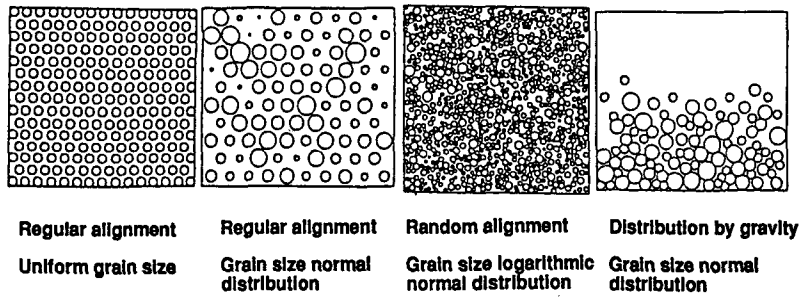

Fig. 2 Various types of initial element alignments.

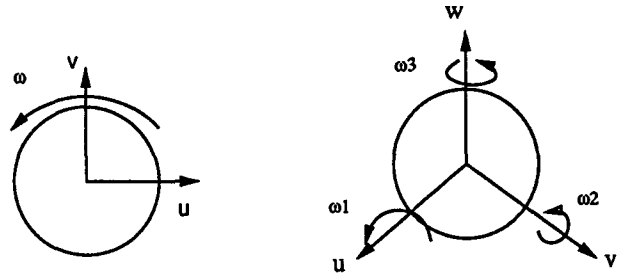

Two dimention Three dimension

Fig. 3 a) Disc and sphere element for a powder particle.

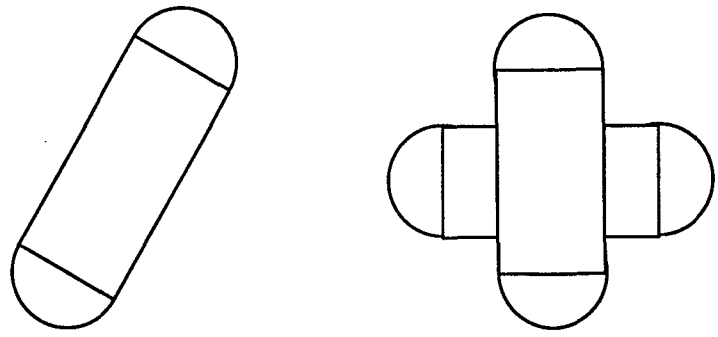

Fig. 3 b) Composite element models for the irregularly shaped and agglomerated powder particles.

The mechanical response of a granular element is considered by parallel and rotational movements through mutual interactions; contact stress transfer is modeled by the generalized stiffness as shown in Fig. 4 for two dimensional situation. Both in the tangential and normal directions on the contact interface are assumed nonlinear spring, dumpers and sliders respectively for elasto-plastic, viscous and frictional components of strains and stresses. In particular, we have developed the micro-compression testing procedure to obtain the load-displacement or the contact stress-strain relation for each grain size particle. As depicted in Fig. 5, an atomized powder particle is pressed upto the specific level of displacements to provide the proper load-displacement relation; due to our experience, the powder particles with grain size from 1 μm to 150 μm can be operated by using WC die and diamond punch for stainless steel gas atomized powders. The linearized stiffness constants in the functional form of grain size are utilized in the following simulations.

For the external action of loading, both velocity displacement vectors for an element can be determined by direct solution of three equations of motion (two in parallel movement and one in rotation) in two dimensional situation. Since some elements have mutual interactions in contact, adequate time marching scheme with time integration algorithm is indispensable to perform precise evaluation of element interactions.

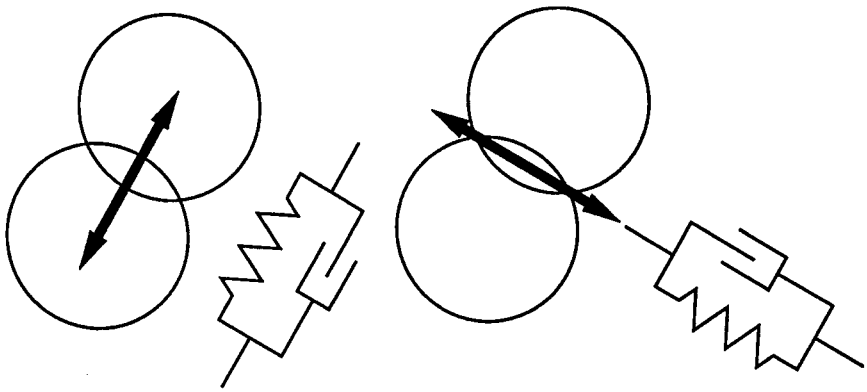

Fig. 4 Generalized stiffness in large defined on the interface between elements.

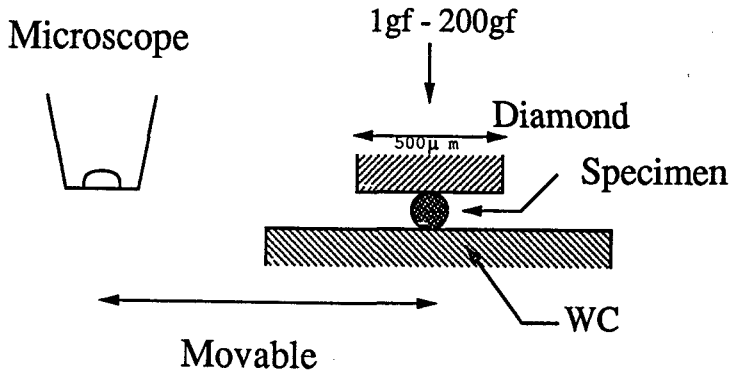

Fig. 5 Microscopic compression testing apparatus to obtain the local load-displacement relation in contact.

Our developing formulation is outlined and summarized in Table 1 to deal with the whole modeling; the following granular simulation system is built on the basis of these strategies and procedures.

GRANULAR SIMULATION SYSTEM

Our developing granular simulation system will be stated with comments on features and functions of model generation, numerical algorithms and model evaluation. The system is divided into three processes: preprocessor, numerical solver and postprocessor.

Preprocessor

Different from such exiting numerical methods as FEM or FDM where quality of element subdivision should be evaluated from the mathematical points of view, the initial element alignment must be discussed through physical aspects of validity. Those are: the initial relative density ρ_R of mass, the average grain size, the grain size distribution, the element allocation, the effect of friction coefficient or the procedure of preliminary compaction. In other words, both the powder particle characterization and the compaction procedure can be taken into account of initial element alignment.

Numerical solver

Three important items must be taken into account in building up necessary formulations and algorithms for numerical solver of granular modeling. **Time marching scheme** should employ two time increment controls: 1) *Global cycle time* to control real time marching with use of average time increment, and 2) *Local sub-cycling* to deal with varying time increments element by element. With respect to **time integration formula**, several algorithms can be selected by analytical sense including accuracy, user friendliness or complexity of target problems. To reduce essential burdens on cpu and memory, data management in **segmentation** should be recommended: interactions among elements should be only considered in their own segmentation or nearest neighboring set of elements.

Postprocessor

Since the simulated results are output in time history, both displacements and velocities are displayed in animation to make understood local and global compaction behaviors directly. In addition to visualization, evaluation of particle movement, rearrangement or flow must be promoted to interpret these calculated data into mechanical parameters: density distribution, porosity coordination numbers and so on. Use of fabric tensor leads to investigation of keys to open frontiers of new powder forming and processing. These functions in postprocessing will be discussed in our coming papers[16,17].

Table 1 List of formulation algorithms to be utilized in the standard granular modeling.

Time Integratio formular

(In case of Euler method)

Relative velocity $\dot{X} = (\dot{x}_2 - \dot{x}_1) - (\dot{\theta}_1 R_1 + \dot{\theta}_2 R_2)$

Normal component of relative velocity $\dot{n} = \dot{X}e$

Tangential component of relative velocity $\dot{s} = \dot{X}t$

Motion equation

Increment of displacement $\Delta n = \dot{n}\Delta t$

$\Delta s = \dot{s}\Delta t$

Increment of contact force $\Delta F_n = K_n \Delta n$

$\Delta F_s = K_s \Delta s$

Load-displacement

Contact force $(F_n)_N = (F_n)_{N-1} + \Delta F_n$

$(F_s)_N = (F_s)_{N-1} + \Delta F_s$

Acceleration $m(x)\ddot{x}_{(x)} = \sum_i F(x)_i$

$I(x)\ddot{\theta}_{(x)} = \sum_i M(x)_i$

Velocity $(\dot{x}_{(x)})_{N+\frac{1}{2}} = (\dot{x}_{(x)})_{N-\frac{1}{2}} + \ddot{x}_{(x)}\Delta t$

$(\dot{\theta}_{(x)})_{N+\frac{1}{2}} = (\dot{\theta}_{(x)})_{N-\frac{1}{2}} + \ddot{\theta}_{(x)}\Delta t$

Time integration

Displacement $(x_{(x)})_{N+1} = (x_{(x)})_N + (\dot{x}_{(x)})_{N+\frac{1}{2}}\Delta t$

$(\theta_{(x)})_{N+1} = (\theta_{(x)})_N + (\dot{\theta}_{(x)})_{N+\frac{1}{2}}\Delta t$

Calculation flow of DBEM

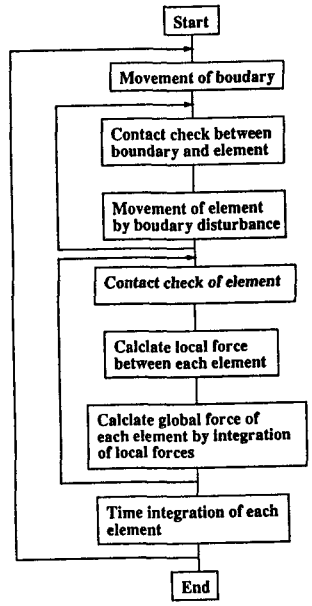

Table 2 Computational conditions in numerical examples.

	Uniaxial Compression	Isotropic Compression	Vibration Compactoin
Tool Size	26.7 X 23.2	26.7 X 23.2	25.0 X 25.0
Number of element	885	885	885
Innitial allocation	Uniform Grain Size Regular alignment	Uniform Grain Size Regular alignment	Grain Size normal distribution Distribution by gravity
Initial relative density	41 %	41 %	81 %
Tool threading speed	3 x 10^{2} / sec	3 x 10^{2} / sec	
Time step	1.0 x 10^{-5}	1.0 x 10^{-5}	1.0 x 10^{-6}
Calculation Cycle	3.0 x 10^{3}	3.0 x 10^{3}	1.0 x 10^{4}

NUMERICAL EXAMPLES

Two types of target problems are taken for numerical examples to demonstrate validity and effectiveness of our developing granular modeling approach: *static compression* both in uniaxial and quasi-isotropic cases and *vibration compaction* with constant frequency and amplitude for the atomized SUS304 powders.

In the static compression simulation is compared the powder particle flow with compaction in two cases: the computational conditions are listed in Table 2. Regular element alignment with uniform grain size is commonly used in both computations. Figs. 6 and 7 show time history of the geometric configuration and the velocity distribution in uniaxial and quasi-isotropic compression, respectively. In both cases, local compaction of particles or arching phenomena are observed at the corner of container in both cases. Due to no friction between elements, agglomeration of porosities is enhanced at the center part in case of the uniaxial compression. While the element particles are still loose at the center for the isotropic compaction. Through these simulations, we have found that both particle and porosity structure should change with reduction in powder forming and that the mass density distribution should be never uniform at least in the intermediate stage of forming.

Here let us state how to generate and distribute elements with the prescribed grain size distribution. To generate the elements with random alignment and prescribed statistic distribution of grain size, Monte-Carlo method and uniform random numbering are both utilized as shown in Fig. 8. In general, the form of statistic grain size distribution is strongly dependent on the powder characteristics of materials; with respect to the grain size, use of logarithmic normal function is recommended in powder characterization. Fig. 9 depicts the logarithmic normal distribution of grain size which is employed in element generation. In this case, the obtained initial element models are shown in Fig. 10 for ρ_R = 30, 40 and 50 %, respectively. In Fig. 11 is shown time history of element configuration and velocity in uniaxial compression for ρ_R = 30 %. Different from uniaxial compression of uniform grain size particles, little agglomeration of porosities can be observed even when no frictions are considered in computation; since smaller element particles infiltrate into gaps between larger elements, porosities are easy to replace with elements.

Finally, let us consider the vibration compaction with constant frequency and amplitude; computational condition is also listed in Table 2. Typical vibration compaction apparatus and dynamic loading signal are respectively shown in Figs. 12 and 13. The same initial element alignment is generated by aaplication of garvity force to the previous alignment which was shown in Fig. 10 for ρ_R = 30 %; in this computation, local friction is considered. Fig. 14 (a) to (d) depicts the change of element alignment and velocity. Since the gravity force is also considered together with vibration, the average center line l_G of gravity is lowered with time. To be noted is agglomeration of powder particle around this line: in particular, larger particles are forced to combine with smaller elements. This agglomeration might be a driving force of uniform compaction in vibration. Furthermore, since the applied external conditions or frequency and amplitude have strong influence on this mechanical behavior, relatively complex responses are expected in general case. Through some basic experiments in vibration, we have found that no compaction takes place below a limit amplitude and that higher flow modes of particle rearrangement are generated in the function of amplitude. The theoretical understanding of these behaviors on the basis of our developing granular modeling will be reported in future.

CONCLUSION

The granular modeling directly describes the mechanical behaviors of powder materials even in processing; the arching or bridging behaviors are understood in thus simulated results where the pores or porosities are locally concentrated and powders agglomerate at the vicinity of container. The effect of grain size distribution for the mixed system of powders is also evaluated in the actual powder forming. To be noted, the present method is applied to quantitative evaluation of both the static and dynamic compression characteristics in actual powder forming, where the compressive load-displacement response is directly estimated through simulation and the dynamic response against the applied frequency and amplitude is calculated to evaluate the uniform consolidation and the vibration induced powder circulation.

Our developing system is still updated to deal with various needs for actual computer aided engineering in practical powder forming [16,17]. Applicability of this system will be investigated in coming papers [18] together with the rational modeling to consider the mechanical behaviors of binders with powders especially in the injection forming; through this study, we can recognize real viscous flowability of metallic powders with binders strongly affected by mechanical interactions between powder particle distribution and true binder viscosity.

References

1] K. Shouji, et al.: Outline of Powder Metallurgy. (1984) Kyouritu.
2] S. Nemat-Nassar et al.: Mechanics of Granular Materials. (1983) Elsevier, 1-8.
3] M. A. Goodman et al.: Arch. Rat. Mech. Anal. (1972) 249-266.
4] Z. P. Bazant et al.: J. Engineering Mechanics. (1983) 1073-1095.
5] S. Shima: J. Materials. (1988) 32-38.
6] O. Cundall: Geotechnique. (1979) 47-65.
7] M. H. Sadd, et al.: Proc. 4th Int. Conf. Comp. Meth. Exp. Meth. (1989) 134-140.
8] C. Thornton et al.: Acta Mech. (1986) 45-61.
9] T. Aizawa and J. Kihara: JSST (1987) 153-158.
10] T. Aizawa and J. Kihara: Proc. 2nd Int. Conf. Computational Engineering and Sciences (1988) 18-ii-1 - 4.
11] T. Aizawa and J. Kihara: Advances in Plasticity (1989) 7-10.
12] T. Aizawa: Computational Techniques for Contact, Impact, Penetration and Perforation of Solids. ASME (1989) 183-190.
13] T. Aizawa, S. Tamura and J. Kihara: Proc. 3rd Int. Conf. Computational Engineering and Sciences (1991)
14] T. Aizawa, S. Tamura and J. Kihara: Mechanical Behavior of Materials. Vol. 3 (1991) 527-532.
15] T. Aizawa: Special Lecture in Society of Materials Sciences (1992).
16] T. Aizawa, S. Tamura and J. Kihara: To be submitted in Journal of Powder Metallurgy (1992).
17] S. Tamura, T. Aizawa and J. Kihara: To be submitted in Proc. Powder Metallurgy World Congress (1992, June, San-Francisco).
18] T. Aizawa, T. Iwai and J. Kihara: To be submitted in Proc. Powder Metallurgy World Congress (1992, June, San-Francisco).

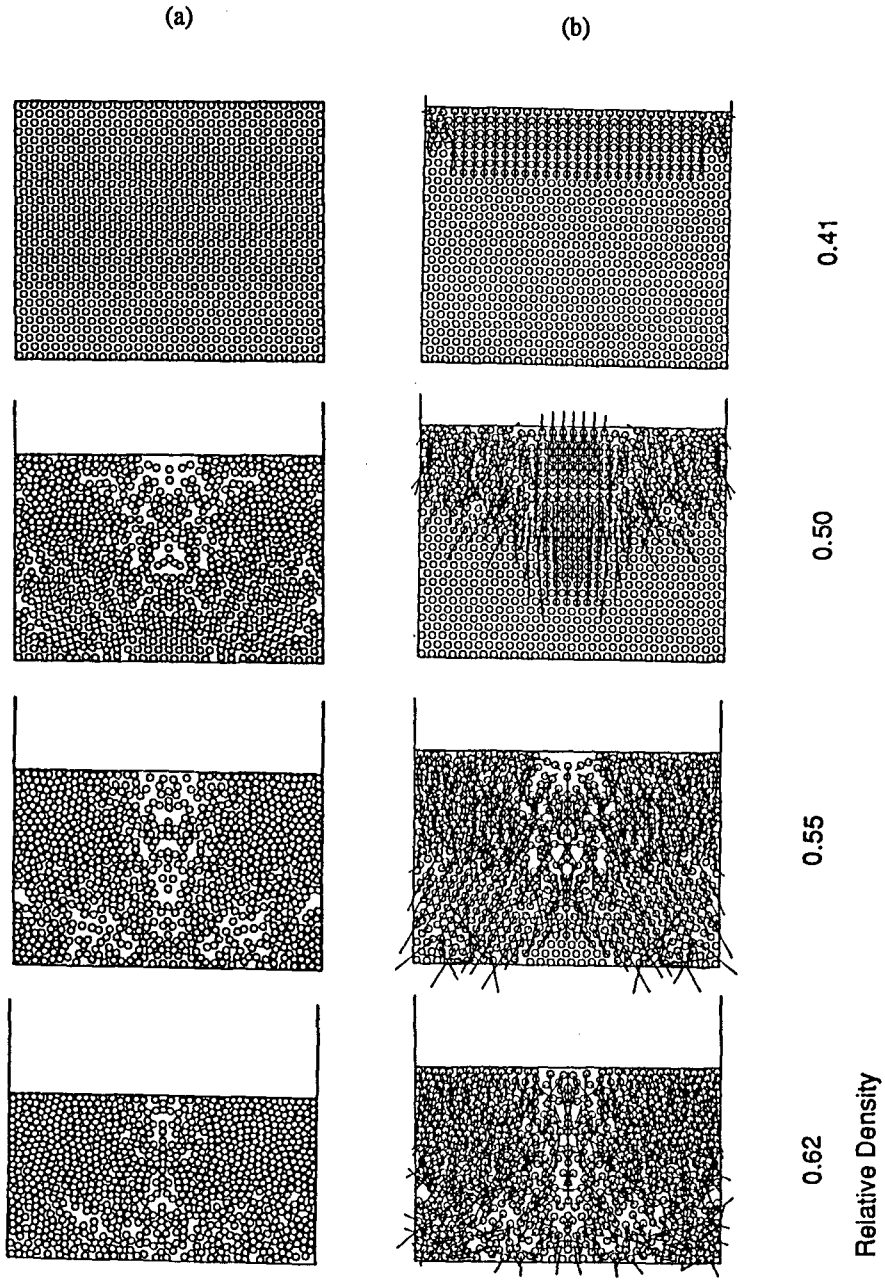

Fig. 6 Time history of the powder element configuration and the velocity distributions with reduction in the uniaxial compression: (a) Change of geometric configuration and (b) Transients of velocity distribution.

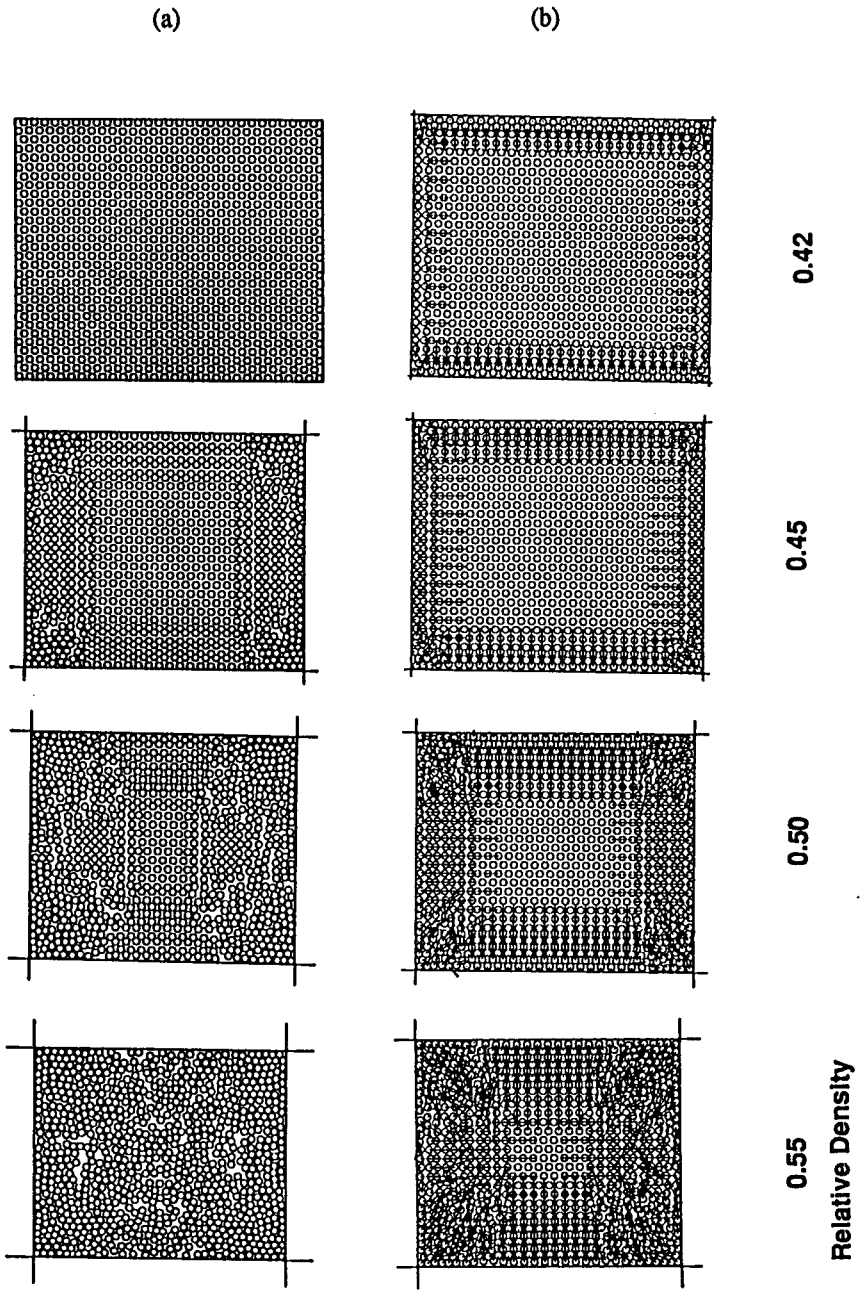

Fig. 7 Time history of the powder element configuration and the velocity distributions with reduction in the quasi-isotropic compression: (a) Change of geometric configuration and (b) Transients of velocity distribution.

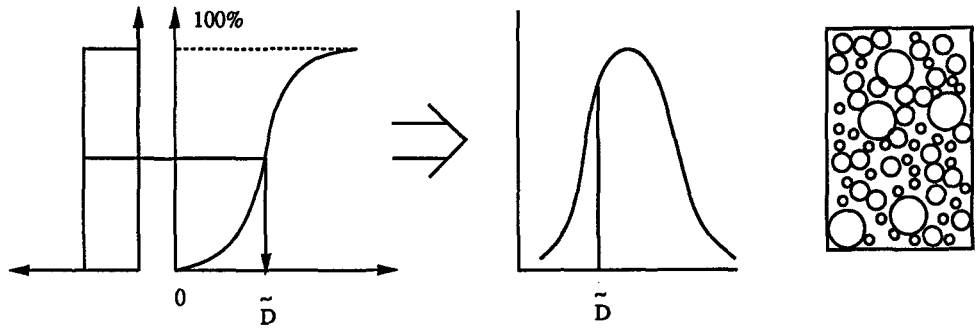

Fig. 8 Generation and alignment of elements with the prescribed statistic distribution of grain size.

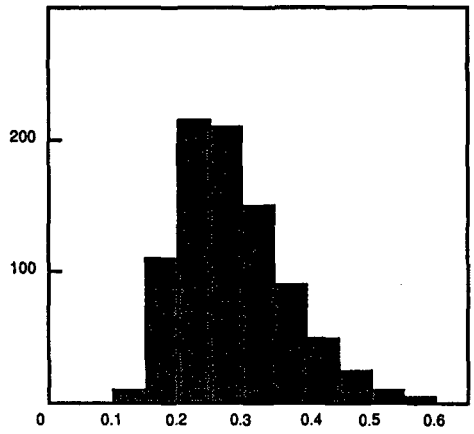

Fig. 9 The logarithmic normal distribution of grain size.

ρ_R = 30 %

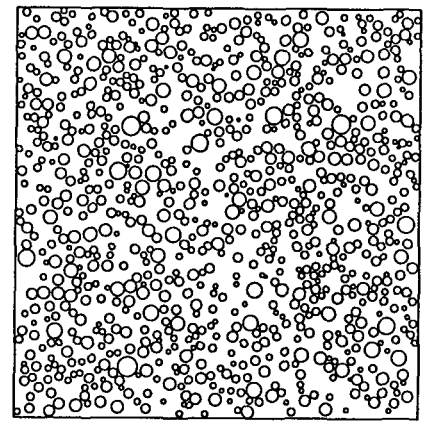

ρ_R = 40 %

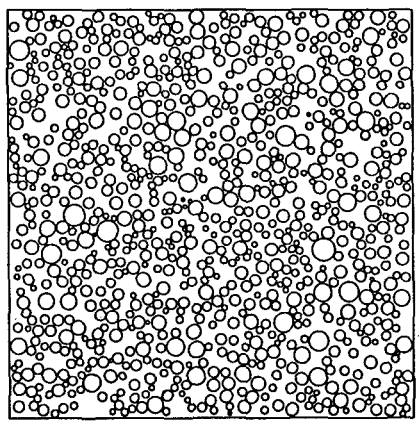

ρ_R = 50 %

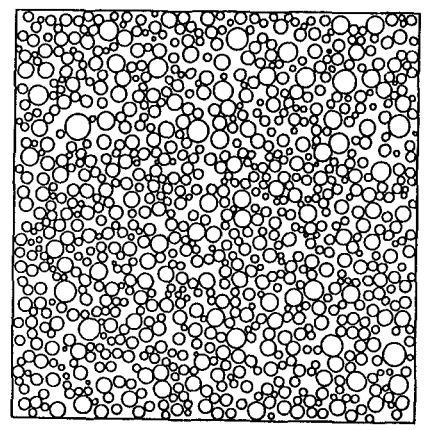

Fig. 10 The initial element alignments with different relative density of mass.

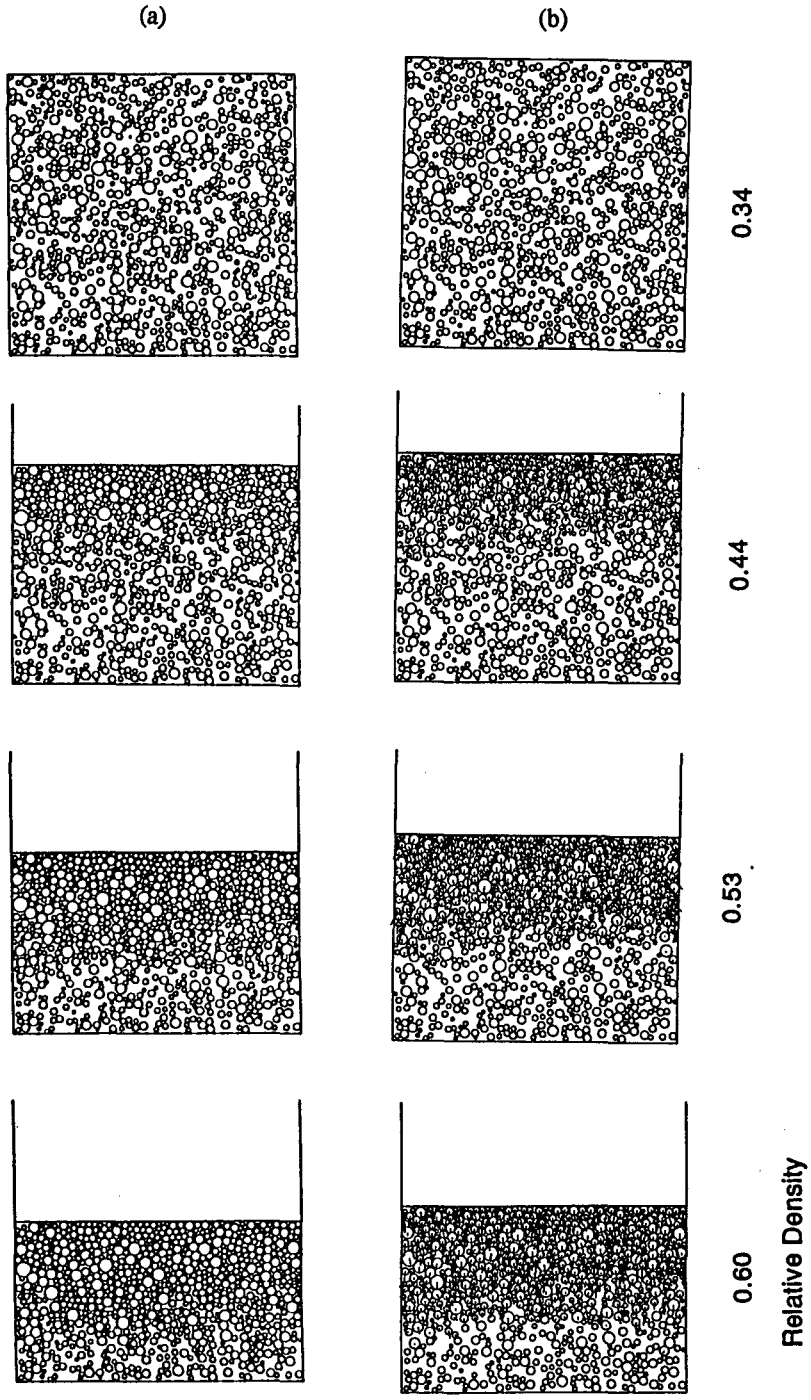

Fig. 11 Time history of the powder element configuration and the velocity distributions with reduction in the uniaxial compression when the initial elements are randomly generated in order to have the logarithmic normal distribution of grain size: (a) Change of geometric configuration and (b) Transients of velocity distribution.

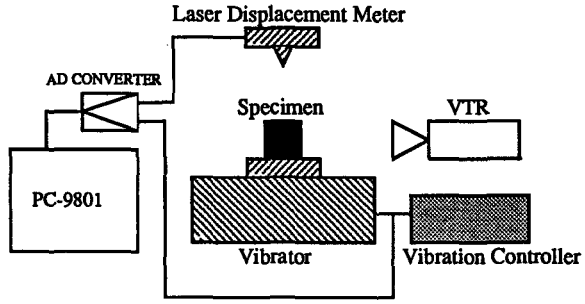

Fig. 12 The schematic view of the vibration compaction procedure.

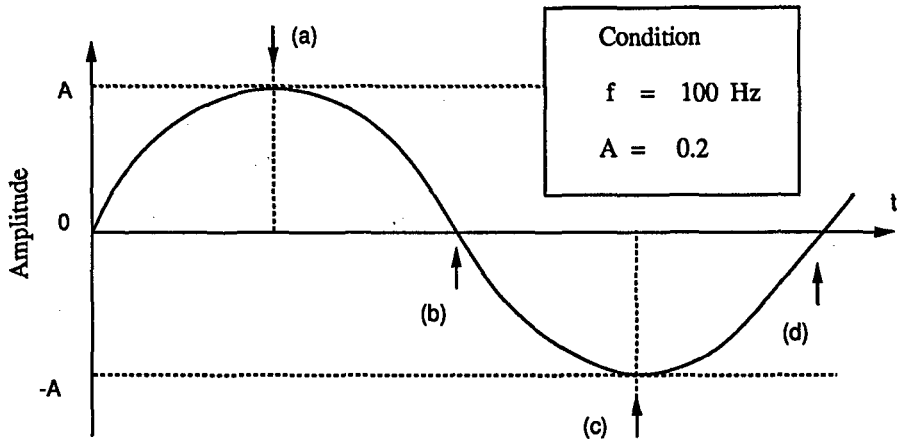

Fig. 13 The action loading signal in the sinusoidal wave.

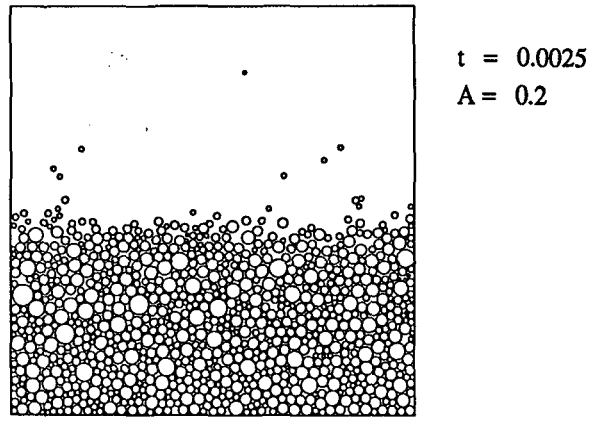

Fig. 14(a) Time response of geometric configuration in vibration.

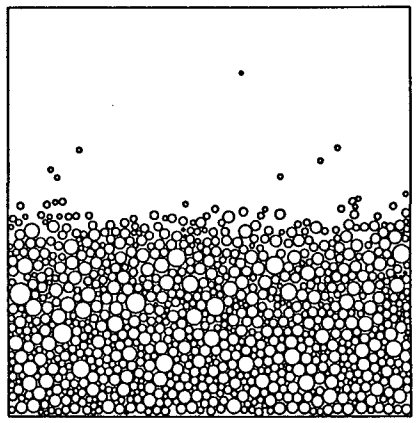

Fig. 14(b) Time response of geometric configuration in vibration.

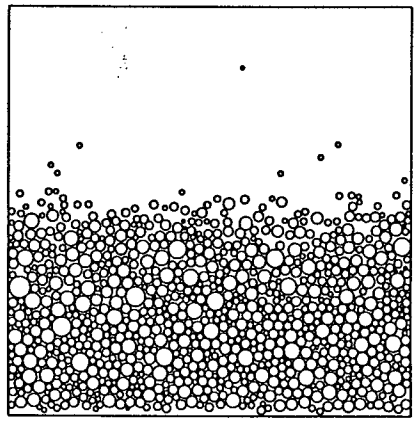

Fig. 14(c) Time response of geometric configuration in vibration.

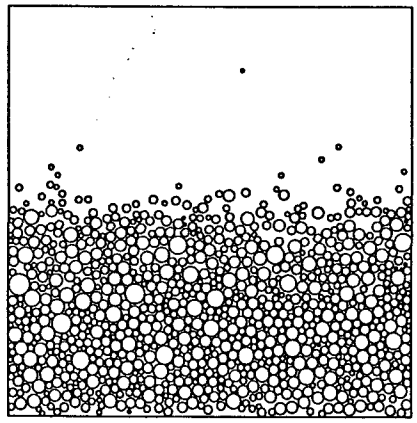

Fig. 14(d) Time response of geometric configuration in vibration.